





# Multi-chamber speckle tracking imaging and diagnostic value of left atrial strain in cardiac amyloidosis

Alberto Aimo <sup>1,2\*</sup>†, Iacopo Fabiani<sup>2†</sup>, Alberto Giannoni <sup>1,2</sup>,  
Giulia Elena Mandoli<sup>3</sup>, Maria Concetta Pastore<sup>3</sup>, Giuseppe Vergaro<sup>1,2</sup>,  
Valentina Spini<sup>2</sup>, Vladyslav Chubuchny<sup>2</sup>, Emilio Maria Pasanisi<sup>2</sup>, Christina Petersen<sup>2</sup>,  
Elisa Poggianti<sup>2</sup>, Claudia Taddei<sup>2</sup>, Vincenzo Castiglione <sup>1</sup>, Sara Latrofa<sup>1</sup>,  
Giorgia Panichella<sup>1</sup>, Carlotta Sciacaluga<sup>3</sup>, Georgios Georgiopoulos<sup>4,5</sup>,  
Claudio Passino <sup>1,2</sup>, Matteo Cameli<sup>3‡</sup>, and Michele Emdin<sup>1,2‡</sup>

<sup>1</sup>Institute of Life Sciences, Scuola Superiore Sant'Anna, Piazza Martiri della Libertà 33, 56124 Pisa, Italy; <sup>2</sup>Cardiology and Cardiovascular Medicine Division, Fondazione Toscana Gabriele Monasterio, Pisa, Italy; <sup>3</sup>Division of Cardiology, Department of Medical Biotechnologies, University of Siena, Siena, Italy; <sup>4</sup>School of Biomedical Engineering & Imaging Sciences, King's College London, St. Thomas' Hospital Campus, London, UK; and <sup>5</sup>Department of Clinical Therapeutics, National and Kapodistrian University of Athens School of Medicine, Athens, Greece

Received 27 July 2021; editorial decision 3 March 2022; accepted 4 March 2022

## Aims

Cardiac amyloidosis (CA) affects the four heart chambers, which can all be evaluated through speckle-tracking echocardiography (STE).

## Methods and results

We evaluated 423 consecutive patients screened for CA over 5 years at two referral centres. CA was diagnosed in 261 patients (62%) with either amyloid transthyretin (ATTR;  $n = 144$ , 34%) or amyloid light-chain (AL;  $n = 117$ , 28%) CA. Strain parameters of all chambers were altered in CA patients, particularly those with ATTR-CA. Nonetheless, only peak left atrial longitudinal strain (LA-PALS) displayed an independent association with the diagnosis of CA or ATTR-CA beyond standard echocardiographic variables and cardiac biomarkers (Model 1), or with the diagnosis of ATTR-CA beyond the validated IWT score in patients with unexplained left ventricular (LV) hypertrophy. Patients with the most severe impairment of LA strain were those most likely to have CA or ATTR-CA. Specifically, LA-PALS and/or LA-peak atrial contraction strain (PACS) in the first quartile (i.e. LA-PALS <6.65% and/or LA-PACS <3.62%) had a 3.60-fold higher risk of CA, and a 3.68-fold higher risk of ATTR-CA beyond Model 1. Among patients with unexplained LV hypertrophy, those with LA-PALS or LA-PACS in the first quartile had an 8.76-fold higher risk for CA beyond Model 1, and a 2.04-fold higher risk of ATTR-CA beyond the IWT score.

## Conclusions

Among STE measures of the four chambers, PALS and PACS are the most informative ones to diagnose CA and ATTR-CA. Patients screened for CA and having LA-PALS and/or LA-PACS in the first quartile have a high likelihood of CA and ATTR-CA.

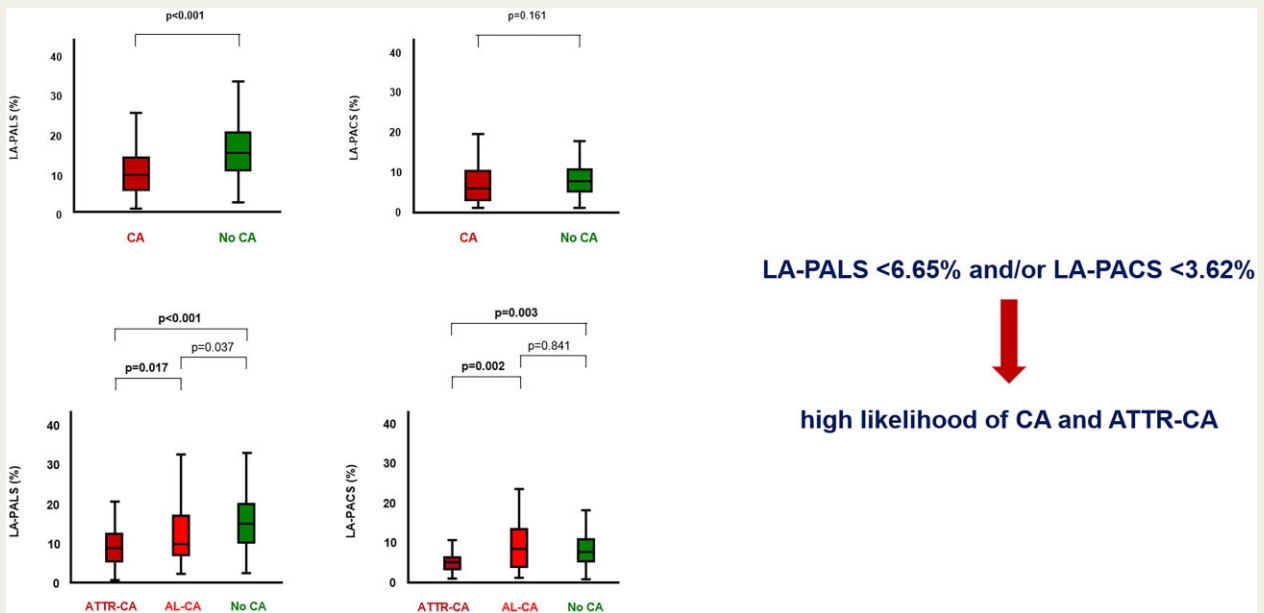
\*Corresponding author. Tel: +39 3477084391. E-mail: a.aimo@santannapisa.it; aimoalb@ftgm.it

†The first two authors contributed equally as first authors.

‡The last two authors contributed equally as senior authors.

Published on behalf of the European Society of Cardiology. All rights reserved. © The Author(s) 2022. For permissions, please email: journals.permissions@oup.com.

## Graphical Abstract



## Keywords

cardiac amyloidosis • echocardiography • speckle-tracking • left atrium • strain

## Introduction

Cardiac amyloidosis (CA) is a disorder characterized by the accumulation of misfolded proteins in the heart as amyloid fibres. Although many proteins can infiltrate the myocardium, immunoglobulin-derived light-chains (AL) and transthyretin (ATTR) alone account for approximately 98% of cases of CA.<sup>1</sup> Most studies have focused on the consequences of amyloid infiltration in the left ventricle, which include a progressive increase of wall thickness and left ventricular (LV) stiffness.<sup>2</sup> Nonetheless, LV dysfunction and amyloid deposition in the left atrial (LA) wall can lead to LA involvement, and right heart chambers can be affected as well.<sup>3</sup>

Transthoracic echocardiography represents the most common and cost-effective tool to evaluate cardiac volumes and function, and is a first-line diagnostic technique in CA.<sup>3</sup> The standard echocardiographic analysis does not allow to reliably identify CA. Recently proposed diagnostic parameters and scores<sup>4</sup> include variables from 2D speckle-tracking echocardiography (STE) to better characterize LV wall motion. STE analysis of the left atrium and right heart chambers is usually feasible and has a low intra- and interobserver variability, but has received very limited attention in CA so far.<sup>5</sup>

LA enlargement is a common finding in CA<sup>3</sup> and has been associated with embolic events and mortality.<sup>6</sup> STE analysis allows to accurately investigate LA functions of reservoir and active contraction, which are impaired in patients with CA than controls even regardless of LA size.<sup>7</sup> As for the evaluation of right heart chambers, it is usually

limited to a small number of parameters, most commonly tricuspid annular plane systolic excursion (TAPSE) and tricuspid annular peak systolic velocity for the right ventricle, and the diameter or area for the right atrium.

We are aware of just two studies exploring all four cardiac chambers through a STE analysis. One was a retrospective, single-centre study evaluating 55 patients with CA, who were compared with patients with hypertrophic cardiomyopathy or healthy controls.<sup>8</sup> Another study evaluated 136 patients with CA, with no control group.<sup>9</sup> In both studies, the Authors performed just an automated calculation of the longitudinal strain (LS) of all chambers from a single apical four-chamber view. Both studies demonstrated the feasibility and reproducibility of LS analysis of the left atrium and right heart chambers in patients with CA, and found a significant impairment of LS values compared with reference values from healthy subjects. However, neither study considered the possible relevance of four-chamber LS for the purpose of the differential diagnosis between CA and mimicking conditions.

In the present study, we investigated for the first time whether a STE analysis extended to the left atrium, right ventricle, and right atrium might hold additive diagnostic value for CA and its subtypes (ATTR- and AL-CA). Specifically, we compared the different strain parameters in their ability to diagnose CA. As parameters of LA strain emerged as strongly associated with CA and ATTR-CA, we investigated its additive value over cardiac biomarkers and variables from standard echocardiography, as well as the validated Increased Wall Thickness (IWT) score.<sup>4,10</sup>



measurements on the same random sample of 50 patients for analysis of inter-observer variability. All contours were drawn again to assess both intra- and inter-observer variability. The main STE parameters are reported in *Figure 1*.

### Left ventricle

2D grey-scale apical four-, two-, and three-chamber views were acquired during three consecutive cardiac cycles, with a frame rate >50 frames/s. The endocardial border was manually traced on an end-systolic frame using a point-and-click approach. The software automatically generated an epicardial line to create the region of interest (ROI) in each apical view (four-, two-, and three chambers), which was manually corrected, when needed. The myocardium was automatically divided into 16 segments. A deformation curve for each segment was generated, and a mean curve was derived from the average of the segments. GLS, ejection fraction strain ratio (EFSR), mass-to-strain ratio (MSR), and septal apical-to-base (SAB) ratio<sup>13</sup> were calculated. Normal GLS values are  $-21.7 \pm 2.5\%$  (lower reference limit  $-16.7$ ) in men and  $-23.0 \pm 2.7\%$  (lower reference limit  $-17.8$ ) in women.<sup>14</sup>

### Left atrium

LA strain analysis was performed on four- and two-chamber apical view grey-scale images and conformed to the dedicated EACVI/ASE document.<sup>5</sup> We adopted the QRS method, whereby the LA endocardial border is manually traced at LV end-systole in both apical views. The software automatically generated a ROI including six segments with different colours per view. The ROI was manually adjusted to include the thickness of the LA myocardium and optimize tracking quality analysis. A curve was generated for each of the 12 atrial segments. Tracking quality was checked and manually corrected, when needed, to ensure optimal tracking; the pulmonary veins and LA appendage were not included. Only segments deemed appropriately and accurately tracked were considered for analysis. The following parameters were calculated as mean between four- and two-chamber measurements:

- (1) peak LA longitudinal strain (LA-PALS), measured during ventricular systole (normal values  $33.5 \pm 10.9\%$ , lower reference limit  $11.7$ )<sup>15</sup> and
- (2) peak LA contraction strain (LA-PACS), measured during atrial contraction (normal values  $15 \pm 5.3\%$ , lower reference limit  $4.4$ ).<sup>15</sup>

We also measured LA strain during the conduit phase by calculating the difference between LA-PALS and LA-PACS.

In patients with atrial fibrillation, flutter, or tachycardia, LA strain analysis was limited to LA-PALS measurement. In this case, all LA strain measurements were carried out on three cardiac cycles and averaged. All analyses were also repeated after excluding patients with atrial fibrillation, flutter, or tachycardia.

### Right ventricle

Right ventricular (RV) myocardial deformation was assessed by 2D speckle-tracking imaging on the RV-focused apical four-chamber view using the Tomtec Arena package. After manual tracing of the end-systolic RV endocardial border, a ROI was automatically generated; its width and position were manually adjusted to include the entire myocardial wall and to exclude the pericardium. Pulmonary valve closure was identified on the pulse-wave Doppler tracing of the RV outflow tract. The software automatically divides the RV free-wall and the interventricular septum. The quality of tracking was automatically validated by software and confirmed visually from the 2D images. Subjects in whom >2 segments per ventricle showed inadequate tracking despite attempts to readjust the

ROI position and width were excluded from analysis.<sup>16</sup> Normal values of RV GLS are:  $-22.3 \pm 3.3\%$  (lower reference limit  $-15.7\%$ ) in men and  $-20.7 \pm 2.9\%$  (lower reference limit  $-14.9\%$ ) in women.<sup>14</sup> For free-wall RV LS, normal values are  $-31.6 \pm 4.0\%$  (lower reference limit  $-27.6\%$ ) in men and  $-29.3 \pm 3.4\%$  (lower reference limit  $-22.5\%$ ) in women.<sup>16</sup>

### Right atrium

The peak right atrial longitudinal strain (RA-PALS) was measured. Endocardial borders of the right atrium were traced on the end-diastolic and end-systolic frame in a focused four-chamber apical view oriented to the right-sided chambers. End-diastole and end-systole were defined based on both electrocardiogram and visual assessment. All images were acquired with a frame rate of at least 50 frames/s. For right atrial (RA) strain measurement, the zero reference was set at end-diastole. As for the left atrium, RA-PALS was measured on three cardiac cycles and averaged were patients had atrial fibrillation, flutter, or tachycardia.

## Statistical analysis

Statistical analysis was performed using IBM SPSS Statistics (version 22, 2013) and Stata (version 16.1). Normal distribution was assessed by plotting a histogram and running the Kolmogorov–Smirnov test. As all variables had a non-normal distribution, they were presented as median and inter-quartile interval. Mean differences among groups were evaluated through the Kruskal–Wallis one-way analysis of variance, applying the Bonferroni correction for multiple comparisons ( $n = 4$ ). Discrete variables were compared by the  $\chi^2$  test with Yates correction or the Fisher's exact test. The strength of correlations was evaluated through the Spearman's rho coefficient. We performed logistic regression analysis to assess the independent association of LA-PALS and LA-PACS with CA and/or ATTR-CA. Model 1 included cardiac biomarkers (NT-proBNP and hs-TnT), and variables from standard echocardiography (LVEF, LVMI,  $E/e'$ , LAVI, and TAPSE). The IWT score, which includes relative wall thickness (RWT)  $>0.6$  (3 points),  $E/e' >11$  (1 point), TAPSE  $\leq 19$  (2 points), GLS  $\geq -13\%$  (1 point), and SAB  $>2.9$  (3 points).<sup>4</sup> Patients with missing data (Model 1, 10%; IWT, 9%; [Supplementary data online, Table S1](#)) were not included in the analysis. We assessed the independent diagnostic value of variables from multi-chamber STE analysis, added one at the time to Model 1: GLS, mass-to-strain ratio (MSR), SAB, LA-PALS/PACS or LA strain during the conduit phase, RV GLS and RA strain. The one-in-ten rule was respected. To increase confidence in our results, we performed bootstrapping with 1000 replicates (i.e. internal validation) and derived 95% bias-corrected bootstrapped CIs. In patients with unexplained LV hypertrophy (defined as septal or posterior wall thickness  $\geq 12$  mm),<sup>4</sup> we examined the additive value of all STE parameters (one at the time) to the IWT score to diagnose CA or ATTR-CA. Multicollinearity was excluded by calculating the variance inflation factor, with a very conservative threshold of 3. Odds ratios (ORs) and corresponding 95% confidence intervals (CIs) were calculated to establish the relative likelihood of CA or ATTR-CA between two patient subgroups. Intra- and inter-observer variability was evaluated through intraclass correlation coefficients and the corresponding 95% CIs. Two-tailed  $P$ -values  $<0.05$  were deemed significant (or  $<0.0125$  after Bonferroni correction).

## Results

### Patient population

Our cohort included 423 patients, with CA confirmed in 261 (62%), and excluded in 162 (38%); the alternative diagnoses are reported in [Supplementary data online, Table S2](#). Patients with CA were more often men, showed higher hs-TnT, an increased

**Table 1** Patient characteristics

	CA n = 261 (62%)	ATTR-CA n = 144 (34%)	AL-CA n = 117 (28%)	No CA n = 162 (38%)	CA vs. no CA P	ATTR- vs. AL-CA P	ATTR-CA vs. no CA P	AL-CA vs. no CA P
Age (years)	78 (72–83)	82 (76–85)	73 (65–78)	79 (74–84)	0.150	<0.001	0.002	<0.001
Men, n (%)	196 (75)	122 (85)	74 (63)	95 (59)	<0.001	<0.001	<0.001	0.437
Systolic arterial pressure (mmHg)	120 (110–140)	130 (115–140)	120 (105–130)	125 (120–140)	0.004	<0.001	0.599	<0.001
NYHA VIII/III/IV, n (%)	51, 127, 77, 6 (2, 20, 30, 49)	28, 67, 46, 3 (2, 19, 32, 47)	23, 60, 31, 3 (3, 20, 27, 51)	44, 69, 47, 2 (1, 27, 29, 43)	0.263	0.797	0.432	0.317
NT-proBNP (ng/L)	4012 (1979–7355)	3516 (1283–7001)	4334 (2099–9121)	2996 (999–5523)	0.026	0.992	0.036	0.093
hs-TnT (ng/L)	59 (38–83)	56 (38–80)	66 (38–133)	42 (26–65)	<0.001	0.202	<0.001	<0.001
eGFR (mL/min/1.73 m <sup>2</sup> )	56 (36–69)	55 (35–68)	56 (37–72)	55 (26–70)	0.440	0.449	0.723	0.299
Atrial fibrillation/flutter/tachycardia, n (%)	83 (61)	68 (47)	25 (21)	62 (39)	0.520	<0.001	0.136	0.002
IVS (mm)	16 (13–18)	17 (15–20)	14 (12–16)	14 (12–15)	<0.001	<0.001	<0.001	0.372
PW (mm)	14 (12–16)	15 (13–17)	13 (11–15)	12 (11–13)	<0.001	<0.001	<0.001	0.040
LVEDVi (mL/m <sup>2</sup> )	50 (42–65)	50 (44–64)	49 (39–68)	60 (51–74)	<0.001	0.492	<0.001	<0.001
LVESVi (mL/m <sup>2</sup> )	23 (18–31)	24 (18–31)	22 (17–32)	24 (17–35)	0.102	0.639	0.187	0.139
LVEF (%)	52 (45–60)	52 (43–56)	55 (48–60)	59 (50–66)	<0.001	0.009	<0.001	0.006
LVMi (mg/m <sup>2</sup> )	148 (121–181)	160 (145–201)	134 (108–158)	135 (114–160)	0.003	<0.001	<0.001	0.091
RWT	0.62 (0.50–0.75)	0.65 (0.55–0.78)	0.55 (0.44–0.69)	0.48 (0.42–0.55)	<0.001	<0.001	<0.001	<0.001
E/e'	16 (12–20)	17 (14–20)	14 (11–19)	13 (10–17)	<0.001	0.001	<0.001	0.470
MR grade (none, mild, moderate, moderate-to-severe, severe), n (%)	2, 104, 103, 40, 9 (1, 3, 15, 40)	0, 50, 59, 27, 6 (0, 35, 41, 19, 4)	2, 54, 44, 13, 3 (2, 3, 11, 38, 46)	3, 59, 57, 31, 3 (2, 19, 35, 36)	0.496	0.103	0.325	0.348
LAD (mm)	46 (42–49)	46 (44–50)	44 (39–48)	46 (42–50)	0.744	<0.001	0.076	0.008
LAVI (mL/m <sup>2</sup> )	43 (35–51)	45 (38–52)	40 (31–47)	41 (36–49)	0.829	0.001	0.056	0.058
RV diameter (mm)	27 (25–30)	27 (26–30)	27 (24–29)	27 (26–30)	0.843	0.055	0.422	0.194
TAPSE (mm)	17 (14–21)	17 (13–19)	19 (14–21)	19 (16–22)	<0.001	0.010	<0.001	0.099
TR grade (none, mild, moderate, moderate-to-severe, severe), n (%)	8, 109, 92, 31, 13 (3, 5, 12, 35, 42)	5, 53, 57, 15, 10 (4, 7, 10, 37, 40)	3, 56, 35, 16, 3 (3, 14, 30, 48)	9, 66, 57, 17, 5 (3, 6, 11, 35, 41)	0.635	0.145	0.449	0.317
Systolic PAP (mmHg)	42 (34–48)	44 (38–48)	39 (30–48)	39 (32–48)	0.622	0.003	0.053	0.169
RA diameter (mm)	45 (40–50)	47 (42–51)	42 (36–48)	43 (40–48)	0.103	<0.001	<0.001	0.224
RA area (cm <sup>2</sup> )	21 (16–24)	22 (18–25)	19 (15–23)	19 (17–23)	0.325	<0.001	0.002	0.084

The Bonferroni correction was applied to account for multiple comparisons (n = 4); significant P-values (<0.0125) are highlighted in bold.

AL, amyloid light-chain; ATTR, amyloid transthyretin; eGFR, estimated glomerular filtration rate; IVS, interventricular septum; LAVI, left atrial volume index; LVEF, left ventricular ejection fraction; LVEDVi, left ventricular end-diastolic volume index; LVESVi, left ventricular end-systolic volume index; LVMi, left ventricular mass index; MR, mitral regurgitation; NT-proBNP, N-terminal pro-B-type natriuretic peptide; NYHA, New York Heart Association; PAP, pulmonary artery pressure; PW, posterior wall; RA, right atrial; RV, right ventricular; RWT, relative wall thickness; TAPSE, tricuspid annular plane systolic excursion; TR, tricuspid regurgitation.



**Table 2** Speckle-tracking echocardiography

	CA		ATTR-CA		AL-CA		No CA		CA vs. no CA		ATTR-CA vs. AL-CA		ATTR-CA vs. no CA		AL-CA vs. no CA	
	n = 261 (62%)	n = 144 (34%)	n = 117 (28%)	n = 162 (38%)	P	P	P	P	P	P	P	P	P	P		
LV																
GLS (%)	-12.1 (-16.7 to -9.0)	-11.8 (-16.4 to -8.5)	-12.4 (-17.3 to -9.3)	-14.6 (-18.5 to -10.7)	<b>0.002</b>	0.135	<b>0.001</b>	0.074								
EFSR	3.3 (2.9-4.1)	3.3 (2.9-3.8)	3.3 (2.9-4.2)	2.5 (1.9-3.1)	<b>&lt;0.001</b>	0.112	<b>&lt;0.001</b>	<b>&lt;0.001</b>								
MSR (%)	22.2 (15.6-32.6)	25.5 (18.8-40.3)	18.4 (12.4-27.8)	18.5 (12.8-24.0)	<b>&lt;0.001</b>	<b>&lt;0.001</b>	<b>&lt;0.001</b>	0.988								
SAB	2.4 (1.2-4.5)	2.5 (1.3-4.6)	2.2 (1.1-4.3)	2.0 (0.9-3.9)	0.114	0.416	0.079	0.381								
IWT score	7 (4-7)	7 (5-7)	6 (3-7)	4 (2-6)	<b>&lt;0.001</b>	<b>0.006</b>	<b>&lt;0.001</b>	<b>&lt;0.001</b>								
LA																
PALS (%)	13.5 (9.6-20.4)	14.0 (10.2-15.7)	13.0 (7.9-21.8)	17.9 (11.6-21.1)	<b>&lt;0.001</b>	0.017	<b>&lt;0.001</b>	0.037								
PACS (%)	6.1 (3.2-10.9)	5.1 (3.1-6.9)	8.4 (3.8-13.5)	7.7 (5.1-14.1)	0.208	<b>0.002</b>	<b>0.003</b>	0.841								
LA strain during the conduit phase (%)	7.0 (4.8-10.1)	8.3 (5.5-9.9)	6.1 (3.5-10.4)	9.5 (6.6-12.4)	0.076	0.306	0.336	0.071								
RV																
GLS (%)	-14.0 (-18.9 to -10.5)	-13.6 (-18.1 to -9.8)	-14.0 (-18.9 to -11.0)	-15.9 (-20.1 to -11.5)	0.039	0.479	0.032	0.207								
Free-wall LS (%)	-14.3 (-19.5 to -9.8)	-13.7 (-18.6 to -9.7)	-14.9 (-20.0 to -10.1)	-14.2 (-20.2 to -9.9)	0.720	0.275	0.858	0.381								
RA																
PALS (%)	9.7 (5.1-17.8)	9.2 (4.6-16.3)	10.8 (7.0-18.4)	12.8 (8.0-20.7)	<b>0.001</b>	0.042	<b>&lt;0.001</b>	0.163								

Significant P-values (<0.0125 after Bonferroni correction) are reported in bold.

AL/ATTR, amyloid light-chain/transferrin; CA, cardiac amyloidosis; IWT, Increased Wall Thickness; LAVI, left atrial volume index; LS, longitudinal strain; MSR, mass-to-strain ratio; PACS, peak left atrial contraction strain; PALS, peak left atrial longitudinal strain; RA, right atrial; RV, right ventricular; SAB, septal apical-to-base longitudinal strain ratio.

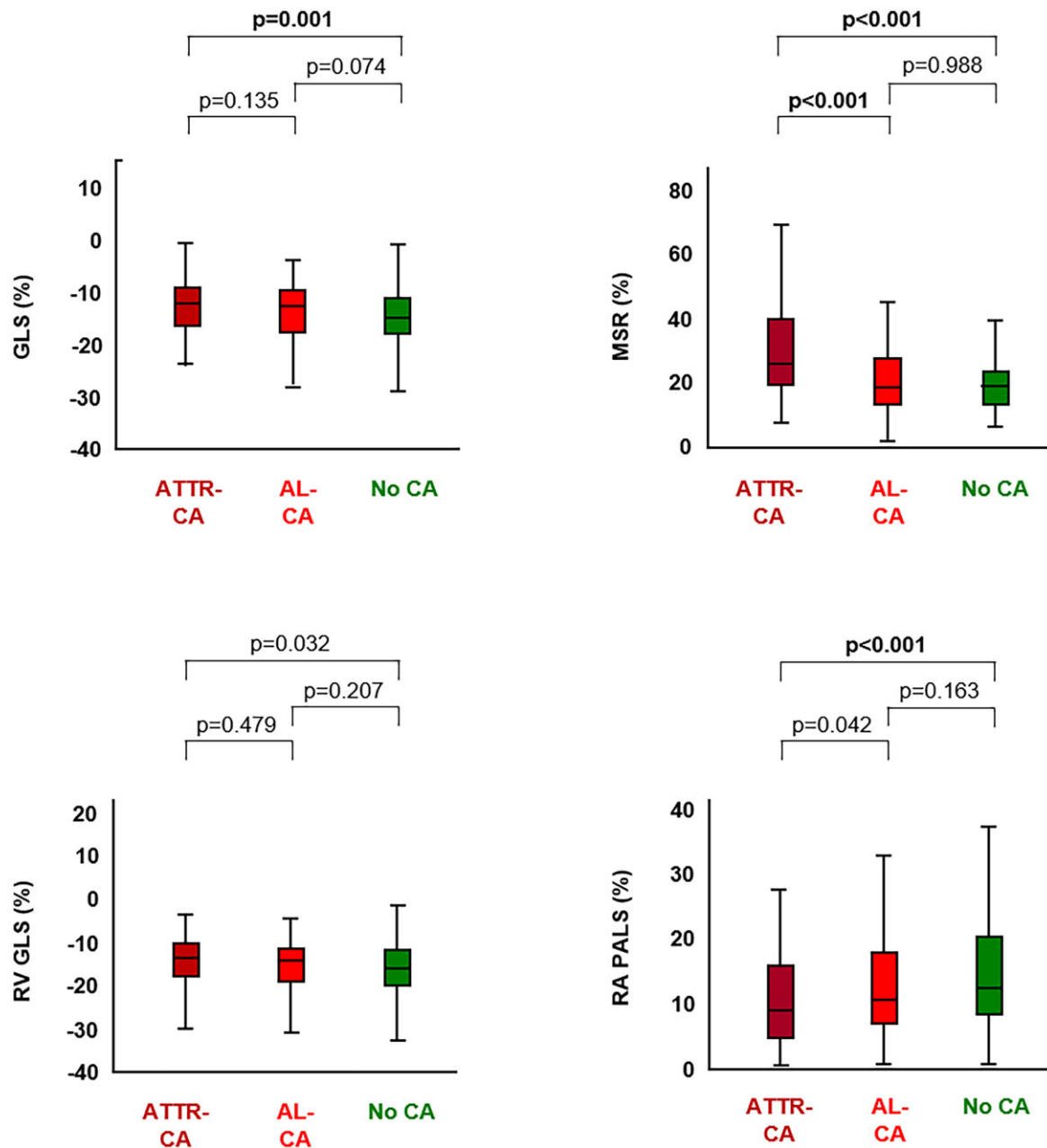


**Figure 2** Left ventricular and right heart strain in patients with amyloid transthyretin (ATTR) or light-chain (AL) cardiac amyloidosis (CA) or without CA. *P* for comparisons between ATTR- vs. AL-CA, ATTR-CA vs. no CA, and AL-CA vs. no CA are reported. Significant *P*-values (<0.0125 after the Bonferroni correction) are reported in bold. GLS, global longitudinal strain; MSR, mass-to-strain ratio; RA, right atrial; RV, right ventricular.

LV mass with a greater impairment of systolic and diastolic function, and a worse RV systolic function than patients without CA. Conversely, the frequency of atrial arrhythmias, LA volume and RA area did not differ significantly (Table 1).

ATTR-CA was diagnosed in 144 patients (34% of the whole population), and AL-CA in 117 (28%). Compared with patients with AL-CA, those with ATTR-CA had a more pseudo-hypertrophic left ventricle with a greater impairment of systolic and diastolic function, more commonly atrial arrhythmias, larger left atrium and right atrium, and a worse RV function (Table 1).

When comparing patients with ATTR-CA vs. those with no CA, the former displayed again a greater LV mass, worse systolic and diastolic function, a larger left atrium and a lower TAPSE. Finally, most measures did not differ significantly between patients with AL-CA and those without CA (Table 1).

### STE analysis

STE analysis was feasible in 98% of cases for left ventricle, 95% for right ventricle, 90% for left atrium, and 85% for right atrium. Reasons for non-analysability were poor acoustic window conditioning the

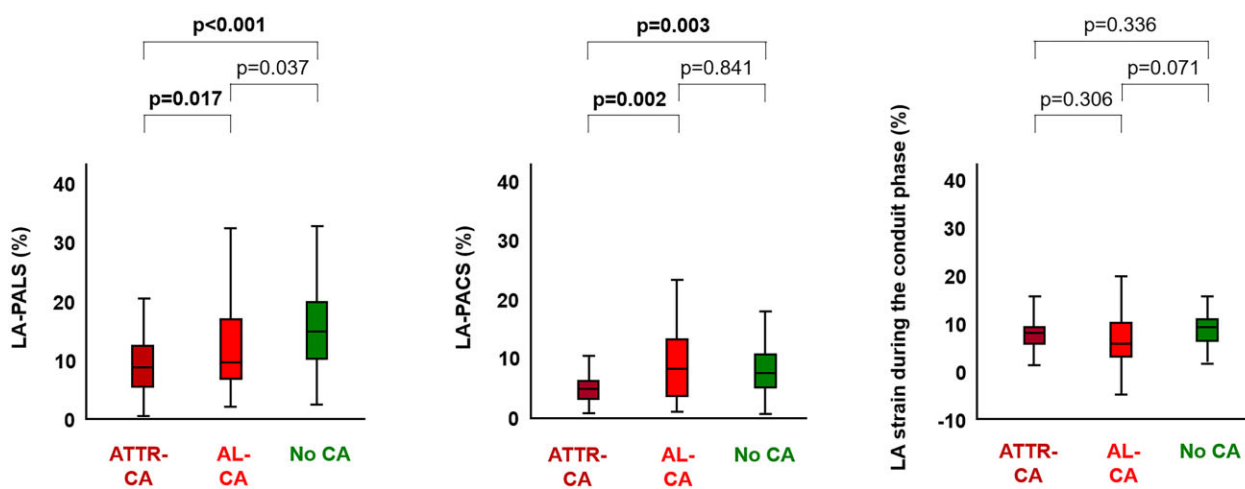


**Figure 3** Left atrial strain in patients with amyloid transthyretin (ATTR) or light-chain (AL) cardiac amyloidosis (CA) or without CA. *P* for comparisons between ATTR- vs. AL-CA, ATTR-CA vs. no CA, and AL-CA vs. no CA are reported. Significant *P*-values (<0.0125 after the Bonferroni correction) are reported in bold. PACS/PALS, peak left atrial contraction/longitudinal strain.

loss of at least two segments, either contiguous or not (left ventricle) or at least one segment (right ventricle), limited visibility because of respiratory motion or excessive lateral wall mobility (right atrium), poor acoustic window limiting the average of peak values between chambers (left ventricle and left atrium). Intra- and interobserver reproducibility was satisfactory, and better for LV and RV parameters than left atrium and right atrium (Supplementary data online, Table S3).

#### Left ventricle

The number of patients with a decreased LV GLS, according to sex-specific lower reference limits of normality (as explained above), was similar in the subgroup of patients with CA and those without (75% vs. 67%,  $P = 0.096$ ). Nonetheless, patients with CA had a lower GLS and EFSR and a higher MSR than those without CA, and these differences were driven by the ATTR-CA subset (Table 2 and Figure 2). IWT score values could be calculated in 363 patients (85%); score values were higher in patients with ATTR-CA than those with AL-CA or no CA (Table 2).

#### Left atrium

LA-PALS was much lower in patients with CA than those without (Table 2), with 67% of patients with CA having LA-PALS lower than the lower reference limit vs. 40% of patients without CA ( $P < 0.001$ ). LA-PALS remained lower in patients with CA after excluding patients with atrial arrhythmias ( $P = 0.002$ ). Differences in LA-PACS and LA strain during the conduit phase were less pronounced and not significant (Table 2).

Patients with ATTR-CA showed lower LA-PALS and LA-PACS values than those with AL-CA or those without CA (Table 2 and Figure 3). This was confirmed in patients without atrial arrhythmias ( $n = 178$ , 68%; Supplementary data online, Table S4).

LA-PALS and LA-PACS correlated with  $E/e'$  and LAVI only in AL-CA patients, while correlations were much less evident in ATTR-CA

patients (Supplementary data online, Figure S1 and Table S5). Furthermore, LA-PALS and LA-PACS correlated with both NT-proBNP and hs-TnT in patients with AL-CA (Supplementary data online, Figure S1 and Table S5).

#### Right ventricle and atrium

Absolute RV GLS was lower in patients with CA than those without (Table 2 and Figure 2). RA-PALS was lower in patients with CA than those without and was particularly depressed in patients with ATTR-CA.

#### Additive diagnostic value of four-chamber STE and LA strain

LA-PALS was the only STE parameter to display an association with CA and ATTR-CA independent of Model 1 both in the whole population and in patients with unexplained hypertrophy, as well as ATTR-CA independent of Model 1 and IWT in patients with unexplained hypertrophy (Table 3). The independent association between LA-PALS and ATTR-CA was confirmed through bootstrapping (Supplementary data online, Table S6).

In the whole population, LA-PALS or LA-PACS in the first quartile (LA-PALS <6.65% or LA-PACS <3.62%) had an OR of 3.60 (95% CI 1.19–10.90) for CA prediction regardless of Model 1, and 3.68 (1.35–10.05) for ATTR-CA. Among patients with unexplained hypertrophy, LA-PALS or LA-PACS in the first quartile had an OR of 8.76 (2.17–35.44) for CA prediction regardless of Model 1, and 2.04 (1.48–2.79) for ATTR-CA independent of the IWT score (Table 3 and Figure 4).

## Discussion

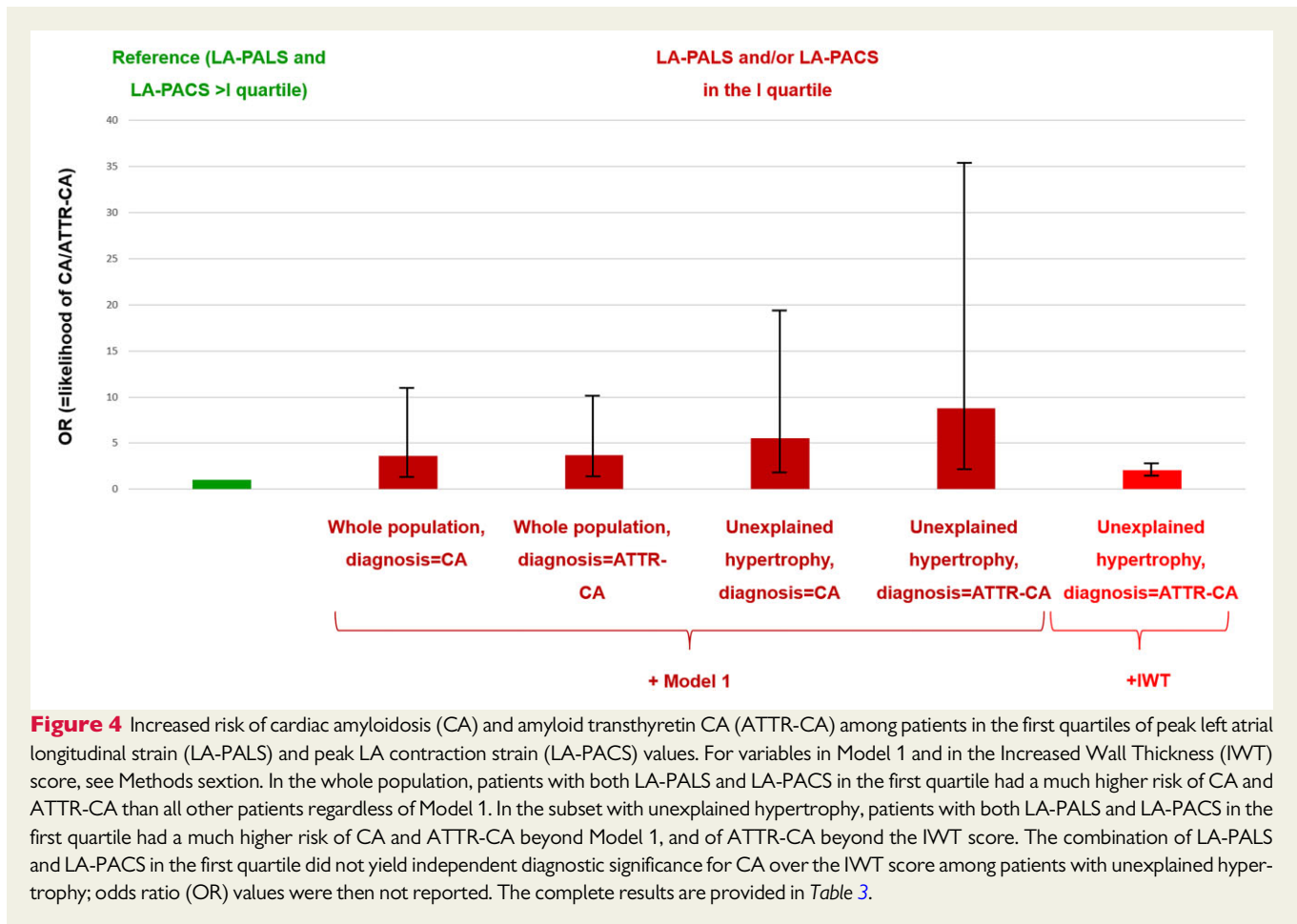
We report that patients with CA have an impaired function of all cardiac chambers compared with patients with CA suspected but ultimately excluded; this difference is mainly driven by patients with



**Table 3** Additive diagnostic value of four-chamber speckle-tracking analysis

	Whole population, diagnosis: CA			Whole population, diagnosis: ATTR-CA			Unexplained hypertrophy, diagnosis: CA			Unexplained hypertrophy, diagnosis: ATTR-CA		
	P	OR (95% CI)	+ Model 1	P	OR (95% CI)	+ Model 1	P	OR (95% CI)	+ IWT	P	OR (95% CI)	+ IWT
LV-GLS	0.678		0.953	0.364		0.108	0.685		0.048		1.06 (1.00–1.13)	
MSR	0.443		0.730	0.795		0.145	0.250		0.004		0.94 (0.90–0.98)	
LV-SAB	0.041	0.97 (0.95–1.00)	0.597	0.035	0.97 (0.95–1.00)	0.004	0.167	0.96 (0.93–0.99)	0.004	0.89 (0.81–0.97)	0.034	0.93 (0.87–0.99)
LA-PALS	0.044	0.94 (0.89–0.99)	0.008	0.006	0.91 (0.85–0.97)	0.331	0.010	0.77 (0.63–0.95)	0.030	0.85 (0.73–0.98)		
LA-PACS	0.133		0.007	0.103		0.609	0.002	8.76 (2.17–35.44)	<0.001	2.04 (1.48–2.79)		
LA-PALS first quartile OR	0.024	3.60 (1.19–10.90)	0.011	0.007	5.56 (1.59–19.42)	0.214						
LA-PACS first quartile												
LA strain during the conduit phase	0.853		0.996	0.530		0.752	0.689		0.540		0.261	
RV-GLS	0.895		0.725	0.634		0.549	0.954		0.131			
RA-PALS	0.242		0.138	0.195		0.261						

For variables in Model 1, see Methods section. For the first quartiles of peak left atrial longitudinal strain (LA-PALS) and peak LA contraction strain (LA-PACS), see Results section. Variables from four-chamber speckle-tracking analysis were added (one at the time) to Model 1 or the Increased Wall Thickness (IWT) score.  
 ATTR, amyloid transthyretin; CA, cardiac amyloidosis; CI, confidence interval; GLS, global longitudinal strain; MSR, mass to strain ratio; OR, odds ratio; RA-PALS, peak right atrial longitudinal strain; RV, right ventricular; SAB, septal apical-to-base longitudinal strain ratio.



ATTR-CA (Figure 5). LA strain is significantly depressed in patients with CA, again particularly in those with ATTR-CA. LA-PALS was associated with CA and ATTR-CA in the whole population independently of a combination of cardiac biomarkers and traditional echocardiographic findings, and also ATTR-CA in patients with unexplained hypertrophy regardless of the IWT score. Similarly, LA-PACS was independently associated with ATTR-CA in the whole cohort and among patients with unexplained hypertrophy. Furthermore, patients with LA-PALS or LA-PACS in the first quartile (<6.65% or <3.62%, respectively) have a much higher risk of CA and ATTR-CA.

Accumulation of amyloid fibres in the heart may cause a direct damage to cardiomyocytes, particularly in AL-CA,<sup>17</sup> and an expansion of extracellular volume by both amyloid and fibrosis, which is particularly prominent in ATTR-CA.<sup>18</sup> These processes may affect all cardiac chambers, as documented by functional abnormalities on non-invasive imaging, results of biopsy specimens in the right ventricle and left ventricle, and forensic examinations. Structural and functional impairment of the left ventricle is usually much more prominent than RV involvement,<sup>3</sup> as confirmed in our cohort, where modest, non-significant differences were found in RV strain parameters between patients with or without CA (Table 2). These findings may be related to a more rapid amyloid accumulation in the left ventricle than in the RV wall. As for the left atrium, the combined effects of changes in LA wall structure and diastolic

dysfunction may explain the profound impairment of LA function in patients with CA compared with patients in whom CA was suspected, but ultimately excluded. LA relaxation and active contraction were particularly affected in patients with ATTR-CA, likely reflecting the slower disease progression and more severe diastolic dysfunction.<sup>7</sup> A profound impairment in LA strain, demonstrated by PALS and/or PACS in the first quartile, was independently associated with ATTR-CA in a cohort of patients with suspected CA. The diagnostic value of LA strain was independent of the combination of biomarkers of LV overload (NT-proBNP), cardiomyocyte damage (hs-troponin T), LV systolic function (LVEF) and diastolic function ( $E/e'$ ), LV mass, LA volume index and RV function (TAPSE). Conversely, even LV MSR, which has been reported to help distinguish between ATTR- and AL-CA,<sup>13</sup> did not hold independent diagnostic value. LA-PALS and LA-PACS even added diagnostic value beyond the IWT score, which incorporates variables from LV STE analysis,<sup>4</sup> and has already been recommended as a possible tool for non-invasive diagnosis of ATTR-CA.<sup>19</sup>

Over the last years, STE has gained increasing importance in CA, and LV strain is currently recommended among the echocardiographic diagnostic criteria of CA by European and American consensus documents,<sup>19,20</sup> both as its absolute value and as systolic longitudinal strain apex-to-base ratio, i.e. the 'relative apical longitudinal strain'. This last has been proposed as an accurate diagnostic

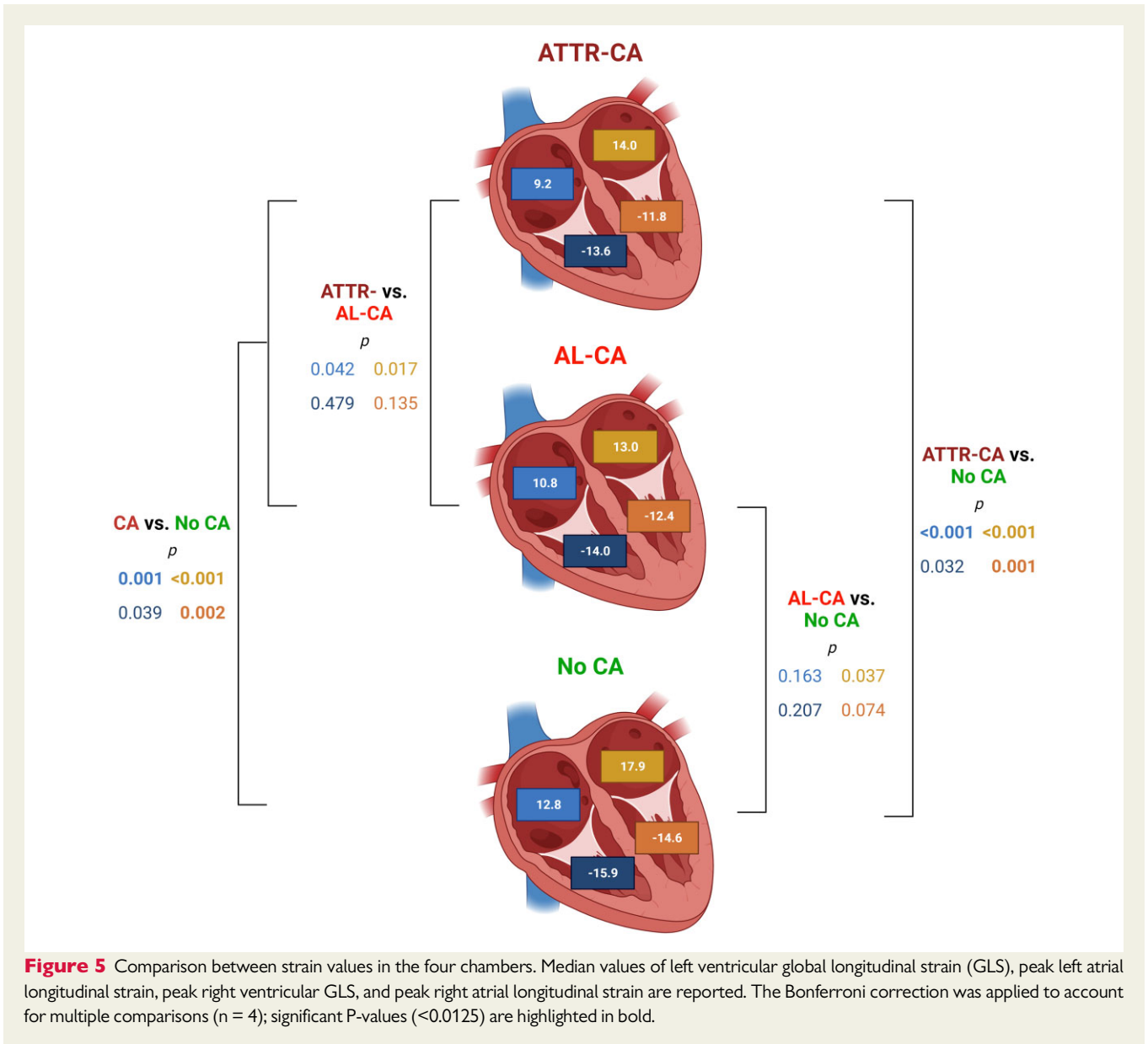


**Figure 5** Comparison between strain values in the four chambers. Median values of left ventricular global longitudinal strain (GLS), peak left atrial longitudinal strain, peak right ventricular GLS, and peak right atrial longitudinal strain are reported. The Bonferroni correction was applied to account for multiple comparisons (n = 4); significant P-values (<0.0125) are highlighted in bold.

measure for CA,<sup>21,22</sup> as well as a prognostic index.<sup>23,24</sup> However, focusing exclusively on LV strain would mean to overlook the early impairment of LV diastolic function and the functional abnormalities in all other cardiac chambers.

LA strain has emerged as a reliable indicator of diastolic function, additive to the usual echocardiographic parameters.<sup>25–28</sup> Therefore, it has been proposed among the most useful indices for the echocardiographic evaluation of heart failure with preserved ejection fraction.<sup>29,30</sup> Some Authors have already focused their research on LA function measured by STE in amyloidosis, founding a significant reduction in patients with CA.<sup>7,31</sup> Importantly, Brand *et al.*<sup>32</sup> have shown that PALS was superior to left ventricle relative apical-to-basal strain ratio in identifying CA patients in a cohort of 54 patients with ‘unclear thick heart pathology’. In this study, we evaluated a much larger cohort of patients evaluated for suspected CA (n = 423), with the alternative diagnoses adjudicated, and an extensive

characterization including clinical and laboratory characteristics. We report that LA strain is profoundly impaired in patients with CA, and particularly in those with ATTR-CA, with additive diagnostic significance over the IWT score, which includes E/E’ and LV GLS. Therefore, LA strain measurement could be used as a screening tool in patients with unexplained hypertrophy. The first quartiles of LA-PALS or LA-PACS can be considered as possible diagnostic cut-offs, most notably in patients with unexplained hypertrophy, given the independent diagnostic value of the combination of LA-PALS <6.65% or LA-PACS <3.62% and its ability to reclassify patient risk of ATTR-CA.

A possible limitation of this study is the arbitrary selection of variables included in Model 1. On the other hand, no diagnostic models have been proposed in patients with suspected CA, with the partial exception of the scores by Boldrini *et al.*,<sup>4</sup> which are to be employed in specific patient subsets (for example, the IWT score in patients

with unexplained hypertrophy). We employed commonly available variables reflecting cardiac damage and the structure and function of multiple chambers. Several patients had not all the variable values for Model 1 or the IWT score, although they were no more than 10%, beyond which statistical analysis may be biased.<sup>33</sup> We avoided to create a diagnostic score based on multi-chamber STE or to integrate LA strain into the IWT score,<sup>4</sup> since this would require a dedicated, and possibly multicentre, study. Another possible development is the validation of our findings in other referral centres for CA or in other settings with a lower observed prevalence of CA. Finally, we deliberately focused on the diagnostic value of STE findings, rather than their prognostic significance.

In conclusion, STE measures of all four chambers are abnormal in patients with CA, particularly in ATTR-CA. LA strain is particularly reduced and holds independent diagnostic significance. Among patients screened for CA, those with LA-PALS <6.65% and/or LA-PACS <3.62% have a high likelihood of CA and ATTR-CA.

## Supplementary data

Supplementary data are available at *European Heart Journal - Cardiovascular Imaging* online.

**Conflict of interest:** none declared.

## Data availability

Original data are available upon reasonable request.

## References

- Benson MD, Buxbaum JN, Eisenberg DS, Merlini G, Saraiva MJM, Sekijima Y et al. Amyloid nomenclature 2020: update and recommendations by the International Society of Amyloidosis (ISA) nomenclature committee. *Amyloid* 2020;**27**:217–22.
- Vergaro G, Aimo A, Barison A, Genovesi D, Buda G, Passino C et al. Keys to early diagnosis of cardiac amyloidosis: red flags from clinical, laboratory and imaging findings. *Eur J Prev Cardiol* 2020;**27**:1806–15.
- Falk RH, Quarta CC. Echocardiography in cardiac amyloidosis. *Heart Fail Rev* 2015;**20**:125–31.
- Boldrini M, Cappelli F, Chacko L, Restrepo-Cordoba MA, Lopez-Sainz A, Giannoni A et al. Multiparametric echocardiography scores for the diagnosis of cardiac amyloidosis. *JACC Cardiovasc Imaging* 2020;**13**:909–20.
- Badano LP, Koliakos TJ, Muraru D, Abraham TP, Aurigemma G, Edvardsson T et al. Reviewers: This document was reviewed by members of the 2016–2018 EACVI Scientific Documents Committee. Standardization of left atrial, right ventricular, and right atrial deformation imaging using two-dimensional speckle tracking echocardiography: a consensus document of the EACVI/ASE/Industry Task Force to standardize deformation imaging. *Eur Heart J Cardiovasc Imaging* 2018;**19**:591–600.
- Mohty D, Petitalot V, Magne J, Fadel BM, Boulogne C, Rouabhi D et al. Left atrial function in patients with light chain amyloidosis: a transthoracic 3D speckle tracking imaging study. *J Cardiol* 2018;**71**:419–27.
- Nochioka K, Quarta CC, Claggett B, Roca GQ, Rapezzi C, Falk RH et al. Left atrial structure and function in cardiac amyloidosis. *Eur Heart J Cardiovasc Imaging* 2017;**18**:1128–37.
- Kado Y, Obokata M, Nagata Y, Ishizu T, Addetia K, Aonuma K et al. Cumulative burden of myocardial dysfunction in cardiac amyloidosis assessed using four-chamber cardiac strain. *J Am Soc Echocardiogr* 2016;**29**:1092–9.e2.
- Huntjens PR, Zhang KW, Soyama Y, Kampaloti M, Lenihan DJ, Gorcsan J III. Prognostic utility of echocardiographic atrial and ventricular strain imaging in patients with cardiac amyloidosis. *JACC Cardiovasc Imaging* 2021;**14**:1508–19.
- Monda E, Palmiero G, Lioncino M, Rubino M, Caiazza M, Dongiglio F et al. External validation of the increased wall thickness score for the diagnosis of cardiac amyloidosis. *Int J Cardiol* 2021;**339**:99–101.
- Gillmore JD, Maurer MS, Falk RH, Merlini G, Damy T, Dispenzieri A et al. Nonbiopsy diagnosis of cardiac transthyretin amyloidosis. *Circulation* 2016;**133**:2404–12.
- Baggiano A, Boldrini M, Martinez-Naharro A, Kotecha T, Petrie A, Rezk T et al. Noncontrast magnetic resonance for the diagnosis of cardiac amyloidosis. *JACC Cardiovasc Imaging* 2020;**13**:69–80.
- Geenty P, Sivapathan S, Stefani LD, Boyd A, Richards D, Kwok F et al. Left ventricular mass-to-strain ratio predicts cardiac amyloid subtype. *JACC Cardiovasc Imaging* 2021;**14**:690–2.
- Park JH. Two-dimensional echocardiographic assessment of myocardial strain: important echocardiographic parameter readily useful in clinical field. *Korean Circ J* 2019;**49**:908–31.
- Cameli M, Miglioranza MH, Magne J, Mandoli GE, Benfari G, Ancona R et al. Multicentric Atrial Strain COmparison between Two different modalities: MASCOT HIT Study. *Diagnostics* 2020;**10**:946.
- Muraru D, Onciu S, Peluso D, Soriani N, Cucchini U, Aruta P et al. Sex- and method-specific reference values for right ventricular strain by 2-dimensional speckle-tracking echocardiography. *Circ Cardiovasc Imaging* 2016;**9**:e003866.
- Martinez-Naharro A, Hawkins PN, Fontana M. Cardiac amyloidosis. *Clin Med (Lond)* 2018;**18**:s30–s5.
- Pucci A, Aimo A, Musetti V, Barison A, Vergaro G, Genovesi D et al. Amyloid deposits and fibrosis on left ventricular endomyocardial biopsy correlate with extracellular volume in cardiac amyloidosis. *J Am Heart Assoc* 2021;**10**:e020358.
- Garcia-Pavia P, Rapezzi C, Adler Y, Arad M, Basso C, Brucato A et al. Diagnosis and treatment of cardiac amyloidosis: a position statement of the ESC Working Group on Myocardial and Pericardial Diseases. *Eur Heart J* 2021;**42**:1554–68.
- Maurer MS, Bokhari S, Damy T, Dorbala S, Drachman BM, Fontana M et al. Expert consensus recommendations for the suspicion and diagnosis of transthyretin cardiac amyloidosis. *Circ Heart Fail* 2019;**12**:e006075.
- Phelan D, Collier P, Thavendiranathan P, Popović ZB, Hanna M, Plana JC et al. Relative apical sparing of longitudinal strain using two-dimensional speckle-tracking echocardiography is both sensitive and specific for the diagnosis of cardiac amyloidosis. *Heart* 2012;**98**:1442–8.
- Robin G, Cognet T, Bouisset F, Cariou E, Méjean S, Pradel S, on behalf of the Toulouse Amyloidosis Research Network Collaborators et al. Value of longitudinal strain to identify wild-type transthyretin amyloidosis in patients with aortic stenosis. *Circ J* 2021;**85**:1494–504.
- Senapati A, Sperry BW, Grodin JL, Kusunose K, Thavendiranathan P, Jaber W et al. Prognostic implication of relative regional strain ratio in cardiac amyloidosis. *Heart* 2016;**102**:748–54.
- Minamisawa M, Claggett B, Adams D, Kristen AV, Merlini G, Slama MS et al. Association of patisiran, an RNA interference therapeutic, with regional left ventricular myocardial strain in hereditary transthyretin amyloidosis: the APOLLO study. *JAMA Cardiol* 2019;**4**:466–72.
- Potter EL, Ramkumar S, Kawakami H, Yang H, Wright L, Negishi T et al. Association of asymptomatic diastolic dysfunction assessed by left atrial strain with incident heart failure. *JACC Cardiovasc Imaging* 2020;**13**:2316–26.
- Inoue K, Khan FH, Remme EW, Ohte N, García-Izquierdo E, Chetrit M et al. Determinants of left atrial reservoir and pump strain and use of atrial strain for evaluation of left ventricular filling pressure. *Eur Heart J Cardiovasc Imaging* 2021;**23**:61–70.
- Cameli M, Sparla S, Losito M, Righini FM, Menci D, Lisi M et al. Correlation of left atrial strain and doppler measurements with invasive measurement of left ventricular end-diastolic pressure in patients stratified for different values of ejection fraction. *Echocardiography* 2016;**33**:398–405.
- Lisi M, Mandoli GE, Cameli M, Pastore MC, Righini FM, Benfari G et al. Left atrial strain by speckle tracking predicts atrial fibrosis in patients undergoing heart transplantation. *Eur Heart J Cardiovasc Imaging* 2021;jeab106. doi:10.1093/ehjci/jeab106.
- Nagueh SF. Heart failure with preserved ejection fraction: insights into diagnosis and pathophysiology. *Cardiovasc Res* 2021;**117**:999–1014.
- Cameli M, Pastore MC, Mandoli GE. Left atrial strain: a key element for the evaluation of patients with HFpEF. *Int J Cardiol* 2021;**323**:197–8.
- Rausch K, Scalia GM, Sato K, Edwards N, Lam AK, Platts DG et al. Left atrial strain imaging differentiates cardiac amyloidosis and hypertensive heart disease. *Int J Cardiovasc Imaging* 2021;**37**:81–90.
- Brand A, Frumkin D, Hübscher A, Dreger H, Stangl K, Baldenhofer G et al. Phasic left atrial strain analysis to discriminate cardiac amyloidosis in patients with unclear thick heart pathology. *Eur Heart J Cardiovasc Imaging* 2021;**22**:680–7.
- Bennett DA. How can I deal with missing data in my study? *Aust N Z J Public Health* 2001;**25**:464–9.